Frontiers of Physics
https://doi.org/10.1007/s11467-019-0950-z
Front. Phys.
15(3), 33201 (2020)

Topical Review

Graphitic carbon nitride based single-atom photocatalysts

Junwei Fu (傅俊伟)[1], **Shuandi Wang** (王栓娣)[1], **Zihua Wang** (王自华)[1], **Kang Liu** (刘康)[1], **Huangjingwei Li** (李黄经纬)[1], **Hui Liu** (刘恢)[2], **Junhua Hu** (胡俊华)[3], **Xiaowen Xu** (徐效文)[1], **Hongmei Li** (李红梅)[1,†], **Min Liu** (刘敏)[1,‡]

[1] *School of Physics and Electronics, State Key Laboratory of Powder Metallurgy, Hunan Provincial Key Laboratory of Chemical Power Sources, Central South University, Changsha 410083, China*
[2] *School of Metallurgy and Environment, Central South University, Changsha 410083, China*
[3] *School of Materials Science and Engineering, Zhengzhou University, Zhengzhou 450002, China*
Corresponding authors. E-mail: †*hongmeili@csu.edu.cn,* ‡*minliu@csu.edu.cn*
Received September 18, 2019; accepted December 4, 2019

Single-atom photocatalysts, due to their high catalysis activity, selectivity and stability, become a hotspot in the field of photocatalysis. Graphitic carbon nitride (g-C_3N_4) is known as both a good support for single atoms and a star photocatalyst. Developing g-C_3N_4-based single-atom photocatalysts exhibits great potential in improving the photocatalytic performance. In this review, we summarize the recent progress in g-C_3N_4-based single-atom photocatalysts, mainly including preparation strategies, characterizations, and their photocatalytic applications. The significant roles of single atoms and catalysis mechanism in g-C_3N_4-based single-atom photocatalysts are analyzed. At last, the challenges and perspectives for exploring high-efficient g-C_3N_4-based single-atom photocatalysts are presented.

Keywords graphitic carbon nitride, single atoms, atomically dispersed sites, site-isolated catalysts, photocatalysis

Contents

1 Introduction

Photocatalysis is one of the potential solutions to energy crisis and environmental pollution [1–3]. Since Wang *et al.* firstly reported graphitic carbon nitride (g-C_3N_4) for photocatalytic hydrogen generation from water splitting [4], as a star photocatalyst, it has been widely used in various photocatalytic reactions [5–13]. However, due to its sluggish surface catalytic rates, insufficient light absorption capacity and high recombination rate of photogenerated electron/hole pairs, the photocatalytic performance is still far from the requirements [14–16]. Various effective modification methods have been applied, such as loading of metal cocatalyst [17–19], doping with heteroatoms [20–22], and compositing with other semiconductors [23, 24]. Generally, metal cocatalyst could easily meet the demands for improving photocatalytic activity of g-C_3N_4, mainly attributing to better separation of photogenerated charge carriers and higher surface catalysis activity of metal active sites [25, 26]. For example, Pt, the most typical noble metal cocatalyst, has been proven to be the most effective cocatalyst of g-C_3N_4 for various photocatalytic application [17, 27]. Unfortunately, the low reserves of noble metals greatly limit their price and widespread applications.

As we know, traditional heterogeneous catalysis plays an important role in driving oil refining, ammonia and fine chemical synthesis [8, 16, 28–30]. Generally, heterogeneous catalysts are composed of metal nanoparticles (especially noble metals, such as Pt, Ru) and metal oxide supports. Only the metal atoms exposed on the surface of metal nanoparticles are active in the catalysis reactions

*Special Topic: Solar Energy Storage and Applications (Eds. Min Liu and Haotian Wang).

[23, 31, 32]. The metal atomic utilization is low, and the actual catalytic activity of metal component has not been fully exploited. Furthermore, the heavy consumption of noble metal greatly increases the cost of heterogeneous catalysts. On this background, single-atom heterogeneous catalysts (SACs) containing metals atomically dispersed as isolated catalysis sites emerge. First, SACs exhibited higher catalytic activity than its counterpoint. Second, single-atom metal sites can achieve nearly 100% atomic utilization, greatly reducing the dosage of metal. Third, the single-atom model can more clearly study the real catalytic effect of the active site, facilitating the study of catalytic mechanisms [28, 29, 33–37].

In recent years, g-C_3N_4-based single-atom photocatalysts have been widely studied [3, 38–42]. Combined with the photo-response characters of g-C_3N_4 and the high catalytic activity of single-atom metal sites, they show great potential in the field of photocatalysis [16]. Single atoms are extremely small in size, resulting in a maximum surface free energy. Strong chemical interactions between the g-C_3N_4 support and single atoms are the key factor in the stability of SACs. g-C_3N_4 is an ideal support material for loading single atoms [36, 40, 41, 43]. The typical two-dimensional (2D) layered structure of g-C_3N_4 brings rich surface loading sites. The adjacent layers are connected by weak van der Waals force, the CN atoms in plane are hybridized with sp^2 to form a highly delocalized π-conjugated system [14]. The presence of lone-pair electrons in two-coordinated N atoms provides an opportunity for coordinating metal atoms. The rich lone-pair electrons of N atoms in the CN heterocycle can confine the highly active single metal atoms, resulting stable g-C_3N_4-based single-atom photocatalysts. Moreover, the modified g-C_3N_4 with more defects can also be good support for single atoms. The defects can play a positive role in the stability of single atoms, which can be ascribed to that the single atoms can be embedded into the defects of supports or bonded with adjacent N atoms. In addition, the physicochemical property of g-C_3N_4 support also changes with the aid of the loaded single atoms. The single atoms on g-C_3N_4 can optimize the band structure of g-C_3N_4, extending optical absorption range. The single metal atom can also accelerate the photogenerated charge separation of g-C_3N_4, which are beneficial for photocatalytic reactions.

In this review, we make a comprehensive review on the progress in the preparation, characterization and application of single atoms modified g-C_3N_4 photocatalysts. We focus on how to accurately characterize the single-atom active sites, and the main roles of the single-atom active site in photocatalytic reactions. This review aims to deepen the understanding of g-C_3N_4 based single-atom photocatalysts, with emphasis on the mechanism of photocatalytic reactions. Some perspectives and challenges on the design of g-C_3N_4 supported single-atom photocatalysts are also presented.

2 Main preparation methods of g-C_3N_4-based single-atom photocatalysts

For the single atoms loaded on g-C_3N_4 support, different synthesis methods will form different microscopic structures and active sites, which will ultimately affect their photocatalytic performance. At present, the widely used methods for preparing single atoms on g-C_3N_4 are wet chemical route, thermal copolymerization, atomic layer deposition and metal molecular complexes (Fig. 1). These methods all have their own convenience and advantages. Each preparation method is described in detail below.

2.1 Wet chemical route

Wet chemical route is the most common method to deposit single atoms on the surface of g-C_3N_4 supports, generally including two important steps: (i) the proper amount of metal precursor is fixed on the surface of g-C_3N_4 supports by means of impregnation, adsorption, coordination bonding, and deposition; (ii) appropriate reduction and activation steps are used to convert the surface-bound precursor into stable mono-disperse atoms on the surface of support. Figure 2 exhibits the typical process of single-atom metal supported on g-C_3N_4 by wet chemical route. The g-C_3N_4 with rich mesoporous can obtain higher surface area for better single-atom metal deposition. Mesoporous g-C_3N_4 (MCN) support was prepared by co-thermo-polymerization of g-C_3N_4 precursor and pore-forming template (such as SiO_2 spheres). Soluble metal salt uniformly adsorbed on the surface of MCN. A $NaBH_4$ reduction method was used for reduction and activation of single-atom metals on MCN [44].

Similarly, Vilé *et al.* [45] prepared mesoporous g-C_3N_4 with high specific surface area (155 m^2/g) by co-thermo-polymerization of cyanamide and colloidal silica. Silica acted as template and pore former was removed after

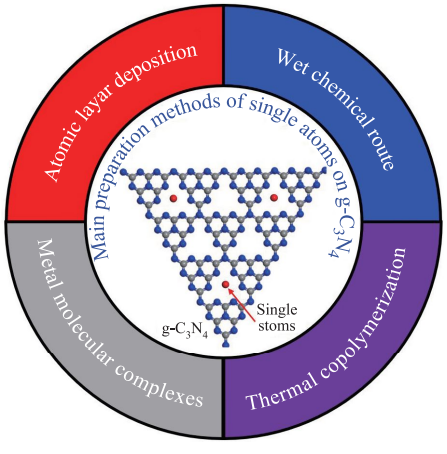

Fig. 1 Main methods for synthesizing single atoms on g-C_3N_4.

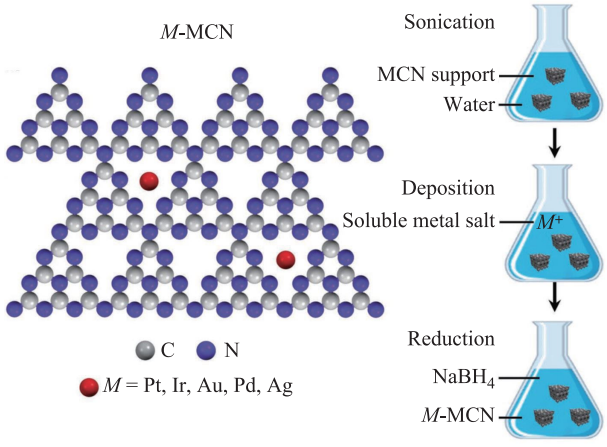

Fig. 2 Typical process of single-atom metal supported on g-C_3N_4 by wet chemical route [44].

thermo-polymerization. The mesoporous g-C_3N_4 was immersed in Pd precursor solution (an aqueous solution of $PdCl_2$ and NaCl), and then $NaBH_4$ solution was used to reduce Pd^{2+} and generate Pd single atom modified mesoporous g-C_3N_4. The different reduction and activation methods of single atoms are important steps in the preparation process. The surface adsorbed metal precursor on g-C_3N_4 can be transformed into single-atom metal by thermal-reduction with inert atmosphere. Tian *et al.* [46] used mesoporous g-C_3N_4 as support for single-atom deposition. The mesoporous g-C_3N_4 was prepared by the same method with Vile *et al.* [45]. Single-atom Ru was anchored on mesoporous g-C_3N_4 by wet-impregnation and thermal-reduction. Specifically, Ru precursor was firstly uniformly adsorbed on mesoporous g-C_3N_4, and then the Ru precursor loaded mesoporous g-C_3N_4 was pyrolyzed at 300°C under N_2 protection. Li *et al.* [47] reported single-atom Pt modified g-C_3N_4 by wet-impregnation deposition with low temperature (125°C) thermal reduction. Firstly, the metal precursor H_2PtCl_6 was uniformly dispersed on the surface of g-C_3N_4 by directly solution evaporation of g-C_3N_4 nanosheets dispersed H_2PtCl_6 solution, and then single-atom Pt was deposited on g-C_3N_4 by thermal reduction under the protection of Ar atmosphere at 125 °C. Reductive atmosphere is also a good strategy for reduction and activation of single-atom metals. Chen *et al.* [48] prepared single-site Au on mpg-C_3N_4 by pre-impregnation $HAuCl_4$ on the surface of mpg-C_3N_4 and a following reduction in H_2/Ar atmosphere at 100°C. Other special method also be developed for reduction and activation of single-atom metals on g-C_3N_4. Liu *et al.* [49] synthesized single-atom Au anchored on g-C_3N_4 by wet-impregnation deposition with amine-induced-reduction strategy. Firstly, the support g-C_3N_4 was ammoniated treated. At the set pH value of the solution, the ammoniated g-C_3N_4 was positively charged, which can electrostatically adsorb $AuCl_4^-$ with negatively charged. Then, the protonated amine can direct reduce Au^{3+} and form Au–N bonds on the surface of g-C_3N_4 support. The different strategies of reduction and activation of single-atom metals on g-C_3N_4 supports in wet chemical route are summarized in Table 1.

The stability of loaded single atoms on the surface of g-C_3N_4 support is an important factor to obtain high-efficient single atoms modified g-C_3N_4 photocatalysts. Though high specific surface area and abundant nitrogen-based ligands make g-C_3N_4 an ideal support for stabilization of single atoms, heteroatoms doping can further enhance the stability of single atoms by ligand interaction between the single atoms and doping atoms. Chen *et al.* [50] firstly exfoliated bulk g-C_3N_4 into g-C_3N_4 nanosheets to get higher specific surface area, and then introduced heteroatom P doping into exfoliated g-C_3N_4 nanosheets. Pd single atoms were loaded on the modified g-C_3N_4 nanosheets by wet-impregnation deposition. The support (P doping modified g-C_3N_4 nanosheets) was firstly impregnated in $Pd(NH_3)_4(NO_3)_2$ solution for complete adsorption of Pd species. Then, the adsorbed Pd species converted into Pd single atoms on the surface of modified g-C_3N_4 nanosheets by microwave-assisted reduction. The modification of heteroatom P doping increased the surface electron density of g-C_3N_4, which reduced the oxidation state of the metal and stabilized the Pd single atoms on g-C_3N_4 by P ligand interaction. In addition to these noble metals single atoms, Liu *et al.* [51] prepared non-noble single-atom Co-based g-C_3N_4 by co-thermal-treatment of $Co(NO_3)_2$ and g-C_3N_4. To stabilize the Co single atoms, phosphidation treatment to form more stable Co_1P_4 on the surface of g-C_3N_4 was performed by co-calcination of $NaH_2PO_2{\cdot}H_2O$ and single-atom Co modified g-C_3N_4.

The confinement effect of supports can effectively prevent the agglomeration of single atoms and improve their dispersion stability. Single atoms dispersed on zeolite [27, 53, 54], mesoporous carbon [55] and metal organic frameworks (MOFs) [1] have been widely studied. These

Table 1 Reduction and activation strategies of single-atom metals on g-C_3N_4 supports in wet chemical route.

Samples	Reduction and activation strategies	Ref.
M@g-C_3N_4 (M = Pt, Ir, Au, Pd, Ag)	$NaBH_4$ solution	[44]
Pd@g-C_3N_4	$NaBH_4$ solution	[45]
Ru@g-C_3N_4	300°C thermal-reduction under N_2 atmosphere	[46]
Pt@g-C_3N_4	125°C thermal-reduction under Ar atmosphere	[47]
Au@g-C_3N_4	100°C thermal-reduction under H_2/Ar atmosphere	[48]
Au@g-C_3N_4	amine-induced reduction	[49]
Pd_1P_4@g-C_3N_4	microwave-assisted reduction	[50]
Co_1P_4@g-C_3N_4	300°C thermal-reduction under Ar atmosphere with NaH_2PO_2	[51]
Pt@g-C_3N_4	icing-assisted photoreduction	[52]
Pt@g-C_3N_4	photoreduction with H_2PtCl_6 aqueous solution dropwise	[17]

supports provided confined pores for single atoms reduction/activation process, which greatly prevented nucleation and crystal growth. During the wet-chemical routes, the nucleation and crystal growth process depend on the diffusion of ions and atoms. Freezing precursor solution to prevent the diffusion of ions and atoms can greatly inhibit the nucleation and growth process. The ice lattice can naturally confine the dispersed single atoms. Wei *et al.* [56] firstly reported synthesis atomically dispersed Pt metal by directly irradiation of freezing H_2PtCl_6 aqueous solution, no support was required. The single-atom Pt was derived from photodecomposition of H_2PtCl_6. Zhou *et al.* [52] prepared single-atom Pt modified g-C_3N_4 by icing-assisted in-situ photocatalytic reduction method [57]. g-C_3N_4 acted as support and provided photogenerated electrons for in-situ reduction of the adsorbed $PtCl_6^{2-}$. Compared with the traditional photo-reduction method, freezing dramatically reduced the size of Pt metal, single-atom Pt can be in-situ deposited on the surface of g-C_3N_4. Similarly, for inhibiting the nucleation and growth of metal during the photo-reduction process, Zhu *et al.* [17] added H_2PtCl_6 aqueous solution into g-C_3N_4 suspension dropwise under visible light irradiation. The addition of H_2PtCl_6 aqueous solution drop by drop greatly prevent the growth of Pt metal grains. Atomically dispersed Pt can be observed on the surface of g-C_3N_4. Noteworthily, the high adding amount of H_2PtCl_6 aqueous solution will lead to big size of Pt nanoparticle, no single-atom Pt can be obtained.

2.2 Thermal copolymerization

Copolymerization of metal precursors and g-C_3N_4 precursors can directly obtain single-atom metal on the surface of g-C_3N_4. Generally, g-C_3N_4 can be easily synthesized by thermal polymerization of carbon, nitrogen-rich small molecules precursors. Oh *et al.* [58] directly thermally treated dicyandiamide and $FeCl_2$ at 600°C for 4 h to prepare single Fe atoms modified g-C_3N_4. As shown in Fig. 3(a), the thermal copolymerization reactions obtained single-atom Fe loaded on g-C_3N_4. The TEM image [Fig. 3(b)] shows arbitrary and nonperiodic morphology of Fe@g-C_3N_4. Figures 3(c) and (d) exhibit the crystalline nature of g-C_3N_4. The introduction of single-atom Fe into g-C_3N_4 did not change the main stacking of heptazine chain layer structure of g-C_3N_4 supports. Li *et al.* [59] reported single Mn atoms located on g-C_3N_4 by direct calcination of the mixture of $KMnO_4$ and urea in an inert gas. Chen *et al.* [60] firstly prepared silver tricyanomethanide (AgTCM) [61, 62] as metal precursors, and then one-step direct calcination of cyanamide, AgTCM and silica at 550°C. After the thermal copolymerization, the silica templates were removed and single-atom dispersed Ag on mesoporous g-C_3N_4 can be obtained. Li *et al.* [63] prepared single-atom Pt or Cu modified g-C_3N_4 by thermal copolymerization of dicyandiamide and metal precursors ($H_2PtCl_6{\cdot}6H_2O$ or $CuCl_2$) at 550°C. Chen *et al.* [44] prepared a series of single-atom metals on g-C_3N_4 by firstly

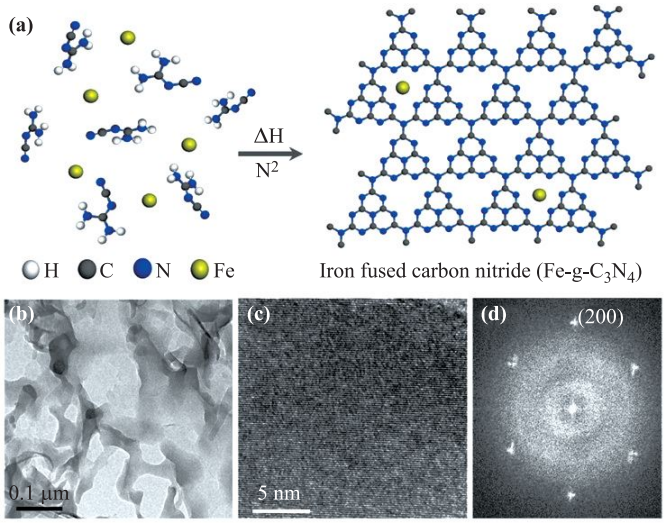

Fig. 3 **(a)** Thermal copolymerization process of metal precursor $FeCl_2$ and g-C_3N_4 precursor dicyandiamide to prepared single-atom Fe functionalized g-C_3N_4. TEM image **(b)** and well-defined local structure **(c)** of single-atom Fe modified g-C_3N_4. **(d)** Selected area electron diffraction electron of g-C_3N_4 (002) orientation [58].

mixture of soluble metal salt precursor, g-C_3N_4 precursor and colloidal silica template. During the process of co-thermo-polymerization, the reducing atmosphere released by g-C_3N_4 precursor can reduce/activate metal salt precursor to obtain single-atom metals. After removal of the SiO_2 template, single-atom metals modified mesoporous g-C_3N_4 can be obtained.

2.3 Atomic layer deposition

Atomic layer deposition (ALD) technique is one of the effective means to accurately deposit single-atom metals on g-C_3N_4 support. Cao *et al.* [64] deposited single-atom Co on the surface of P-doped g-C_3N_4 (PCN) by ALD using cobalt bis(cyclopentadienyl) (Cp) as metal precursor. As shown in Fig. 4(a), the support (PCN) was prepared by phosphidation treatment of pure g-C_3N_4. ALD can anchor atomic Co on PCN with residual surface Cp ligand due to the unsaturated two-coordinated N atoms. Further O_3 treatment eliminated excess Cp ligands. The whole treatment process did not change the main morphology and structure of g-C_3N_4 [Fig. 4(b)]. High-angle annular dark-field scanning transmission electron microscopy (HAADF-STEM) images [Figs. 4(c) and (d)] exhibit the stable single-atom Co on the surface of PCN.

2.4 Metal molecular complexes

Metal atoms in the metal molecular complexes are protected by the surrounding ligands, are another form of atomically dispersed metal site. Compositing metal molecular complexes with g-C_3N_4 have been studied for improv-

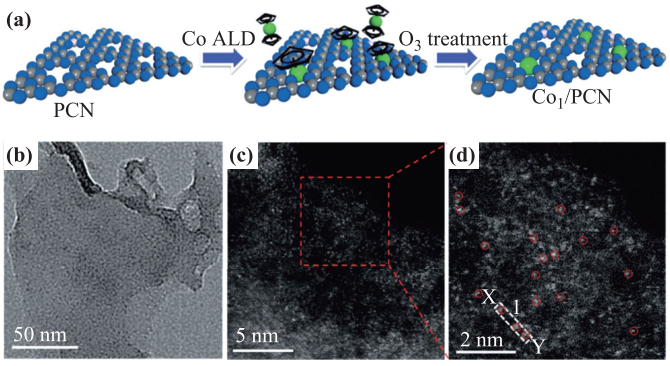

Fig. 4 **(a)** Illustration of the synthesis process of single-atom Co on the surface of P-doped g-C_3N_4 by ALD and O_3 treatment. **(b)** TEM and **(c)** HAADF-STEM images of single-atom Co on PCN. **(d)** magnification image of (c). The red circles in **(d)** represent atomically dispersed Co atoms [64].

ing the photocatalytic performance of g-C_3N_4 [65–67]. Kumar *et al.* [65] reported cobalt phthalocyanine grafted to g-C_3N_4 by simple adsorption effect. As shown in Fig. 5, CoPc with surface –COOH and g-C_3N_4 were firstly synthesized separately. Phthalocyanine molecules are easily agglomerated due to their strong π–π interactions. Increasing the dispersion to reduce the agglomeration is an important strategy to realize the metal single-atom dispersion. The obtained CoPc-COOH and g-C_3N_4 were mixture and stirred in N, N-dimethylformamide (DMF) solution due to the good dispersion of CoPc-COOH in DMF. The adsorbed CoPc-COOH on the surface of g-C_3N_4 can be obtained, and atomically dispersed Co site on g-C_3N_4 greatly improved the selective photocatalytic conversion of CO_2 to methanol. Concentrated sulfuric acid is another dispersion solvent of phthalocyanine molecules. Shi *et al.* [66] prepared iron(II) phthalocyanine (FePc) composited with g-C_3N_4 by easy exfoliation and adsorption method. In order to get good dispersion and close contact of FePc and g-C_3N_4. Concentrated sulfuric acids were used as dispersion solvents, both FePc and g-C_3N_4 nanosheets can be obtained and composited by the exfoliation and adsorption effects.

Summing up, in order to get single-atom metals loading on the g-C_3N_4 support, the metal precursor should firstly uniformly adsorb on the surface of g-C_3N_4-based support or g-C_3N_4 precursor. Then, various post-treatments are used to reduce/activate and anchor single-atom species on the supports. The low loading amount of metals and high specific surface area of g-C_3N_4-based supports are necessary conditions to obtain single-atom metals supported on g-C_3N_4 photocatalysts [44].

Although there are many methods to prepare single-atom photocatalysts, their low yield and low metal loading greatly limit their practical applications. Large-scale preparation of single-atom photocatalysts with high metal loading is still difficult [50, 68–70]. Yang *et al.* [70] reported a universal ligand mediated method for large scale synthesis of transition metal single atom catalysts on carbon black support. The obtained carbon-supported metal single atom catalysts are >1 kg scale. Zheng *et al.* [68] reported an ion adsorption process to prepare earth-abundant Ni single-atom catalysts on commercial carbon black with gram scale. Chen *et al.* [50] studied the scalability of single-atom catalysts on g-C_3N_4. The choice of precursor, synthesis condition, thermal exfoliation time, and metal deposition method is the key criteria for large-scale preparation and application of g-C_3N_4 based single-atom photocatalysts.

3 Strong characterizations of single-atom sites

How to determine the existence and spatial distribution of single atom on the support is the key to understand and

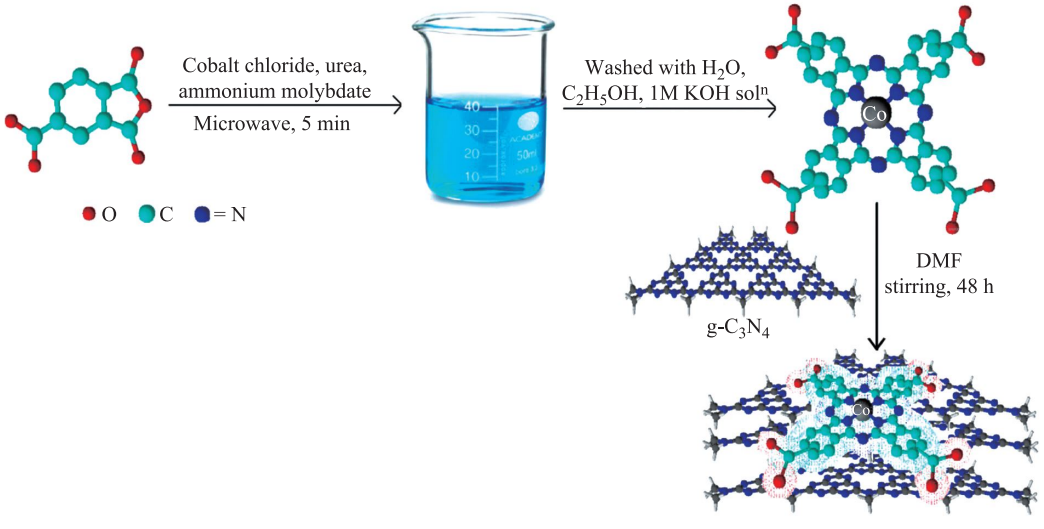

Fig. 5 Synthesis process of CoPc and CoPc modified g-C_3N_4 photocatalyst [65].

develop single-atom photocatalysts. The most intuitive and convincing tool is electron microscopy techniques, such as HAADF-STEM with spherical aberration correction, which can directly observe the morphology and subnanoscale size of single atom [46]. Tian *et al.* [46] performed aberration-corrected (AC) HAADF-STEM measurement to direct analyze the morphology and size of single-atom Ru loaded on g-C_3N_4. As shown in Fig. 6, many small bright spots are uniformly dispersed on the surface of g-C_3N_4 support. These bright spots can be ascribed to Ru atoms due to the Z-contrast difference of Ru atoms and C/N atoms. The ultra-small size of Ru atom indicated that Ru atoms are atomically dispersed.

Three-dimensional (3D) atom probe tomography (APT) technology with atomic resolution can also directly identify the presence and uniform dispersion of single atoms [71]. Jiang *et al.* [71] used 3D APT technology to directly identify the single-atom Ni sites in graphene support. As shown in Fig. 7, each pixel represents one single atom. The distance between different atoms can be obtained directly, so the coordination environment of metal atoms can be analyzed. Figure 7(c) exhibits the statistics of the surrounding coordination of Ni atoms, further proves the presence of single-atom Ni atoms.

X-ray absorption near edge structure (XANES) spectroscopy, and extended X-ray absorption fine structure spectroscopy (EXAFS) can directly determine the chemical state and coordination environment of atoms with high sensitivity [47]. Li *et al.* [47] reported single-atom Pt as cocatalyst on the surface of g-C_3N_4 (Pt-CN)for photocatalytic H_2 generation. The Fourier transforms (FT) EXAFS curves shown in Fig. 8(a) prove that no Pt–Pt bonds can be detected in sample, only obvious Pt–C/N signal can be observed, further confirming the presence of single-atom Pt. Figures 8(b) and (c) determine the possible structural models of Pt-CN by the fitting of experimental EXAFS data.

Infrared spectroscopy with appropriate probe molecules, such as CO, NO, NH_3, and pyridine, can also be used to assess the existence of single metal atom [72, 73]. The content percentage of single metal atom dispersed on the surface of support can be quantitatively analyzed. Ding *et al.* [73] used infrared spectroscopy to fast and conveniently characterize the single-atom Pt on mesoporous zeolite HZSM-5. The stretching frequencies of CO when adsorbed to different Pt species sites are different. Single-atom Pt coordinated with O atoms of supported will result in a cationic charge state of Pt. The stretching frequency of CO adsorbed to single-atom Pt will exhibit higher wavenumber than CO adsorbed to Pt nanoparticles. As shown in Fig. 9, two different absorption bands can be observed, which can be ascribed to CO on single-atom Pt and linear CO on Pt nanoparticles. Moreover, higher Pt loading can lead to more Pt nanoparticles, and higher FTIR intensity of CO adsorbed to Pt nanoparticles. The ratio of absorption band areas can quantitatively identify the ratio of single-atom Pt to Pt nanoparticles.

Other characterizations can also indirectly characterize the existence of single atoms. For example, the absence of Pd XRD reflection peak indicated the high dispersion

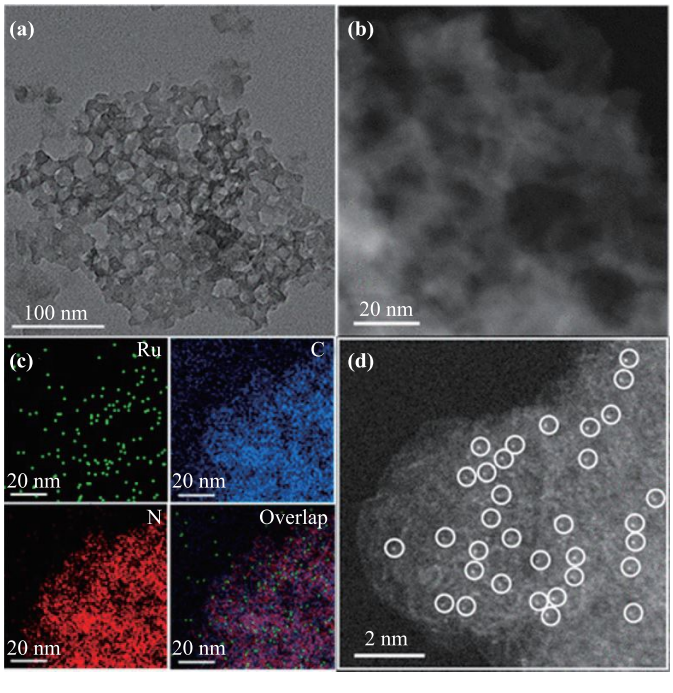

Fig. 6 TEM **(a)** and HAADF-STEM **(b)** images of the Ru loaded on g-C_3N_4 sample. **(c)** EDX element maps of Ru, C, and N atoms on the Ru loaded on g-C_3N_4 sample. **(d)** AC HAADF-STEM images of the Ru loaded on g-C_3N_4 sample [46].

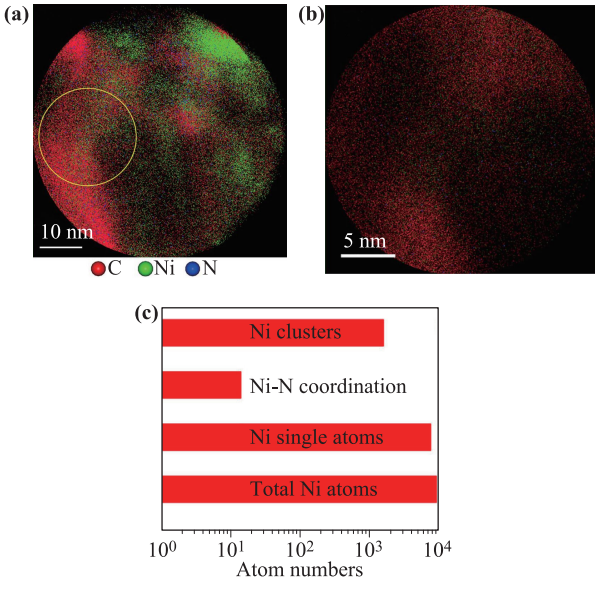

Fig. 7 **(a)** 2D atom map of Ni atom modified N-doped graphene. **(b)** Enlarge atom map of the yellow circle shown in (a). **(c)** The statistics of Ni atom in the selected area shown in (b) [71].

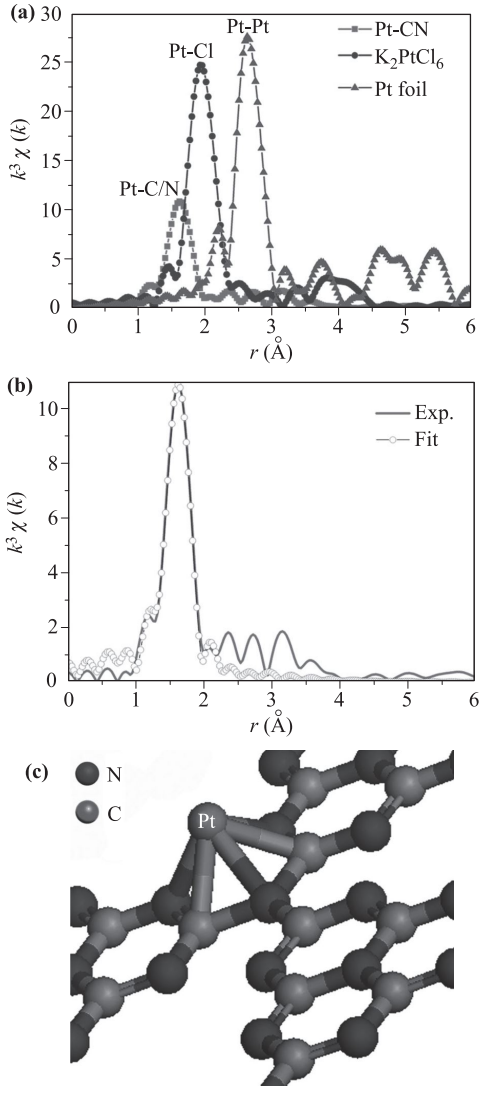

Fig. 8 **(a)** Fourier transform EXAFS curves of the Pt L3-edge oscillations of Pt-CN, K_2PtCl_6, and Pt foil. **(b)** Experimental data and the fitting curves of the Pt-CN. **(c)** The possible schematic models of Pt-CN [47].

of Pd [50], which is necessary for single Pd atom dispersed on g-C_3N_4. The stable existence of single atoms requires strong interaction between single atoms and supports, which makes it impossible for single atoms to exist in zero valence state. Using X-ray photoelectron spectroscopy (XPS) to analyze the valence state of metal atoms is also a good indirect method [50].

4 Main roles of single atoms on g-C_3N_4 in photocatalytic reactions

For an excellent photocatalyst, activity, selectivity and stability are three important factors that must be considered. The low photocatalytic activity of g-C_3N_4 can be attributed to: i) insufficiency light absorption performance;

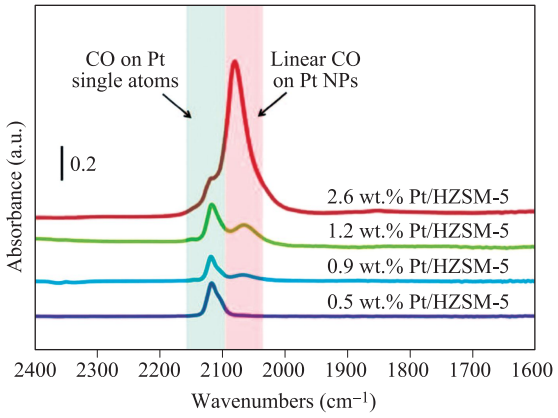

Fig. 9 FTIR spectra of CO adsorbed at Pt/HZSM-5 with different Pt loading [73].

ii) sluggish surface catalytic kinetics; iii) low utilization efficiency of photogenerated charge carriers. Single-atom metals on the surface can act as efficient active sites for catalysis reactions, which greatly improve the reaction kinetics. Moreover, the intrinsic properties of g-C_3N_4 can be changed by the loading of single-atom metals, so that the effect of light absorption and separation of photogenerated charge carriers can be improved.

Generally, only N atoms in g-C_3N_4 can bond with metal atoms due to the unsaturated coordination of N atoms. Three types of N atoms can be used to interact with metal atoms, namely two-coordinate N (N–C_2), tri-coordinate N (N–C_3) and surface amino N (N–H_x). The local bond coordination of single atom metals at g-C_3N_4 interface is important structure factor to analyze the photocatalytic performance. Oh *et al.* [58] proved the coordination of divalent Fe atom in g-C_3N_4 by detailed experimental and computational evidences. Solid-state nuclear magnetic resonance (NMR) spectroscopy of g-C_3N_4 and Fe modified g-C_3N_4 (Fe-g-C_3N_4) are shown in Fig. 10. Clearly, no obvious difference can be observed in the ^{13}C spectra [Fig. 10(a)]. Just the chemical shift of ^{15}N in Fe-g-C_3N_4 changed in peak 3 region (from 165.3 to 160.9 ppm) compared with the pure g-C_3N_4. Cross-polarization magic angle spinning (CP-MAS) NMR spectroscopy [Figs. 10(c) and (d)] were used to further determine the attribution of the peaks. As indicated in the chemical structure diagram of g-C_3N_4 [Fig. 10(d)], The peaks labeled with different colors correspond to atoms of different colors in g-C_3N_4. The signals of peak 3 regions come from two-coordinate N [N atoms in the red circle in Fig. 10(d)] in the g-C_3N_4 structure. The NMR characterizations confirmed that Fe atoms coordinated with two-coordinated N atoms. Further theoretical calculation proved that the cavities of g-C_3N_4 were the most favorable Fe adsorption sites with strong binding energy. The Fe single atoms coordinated with two-coordinated N in the cavities of g-C_3N_4. Similarly, Li *et al.* [59] proved metal atoms bond with the surface amino N (N–H_x) to form N_H–Mn^{II} in single atom Mn modified

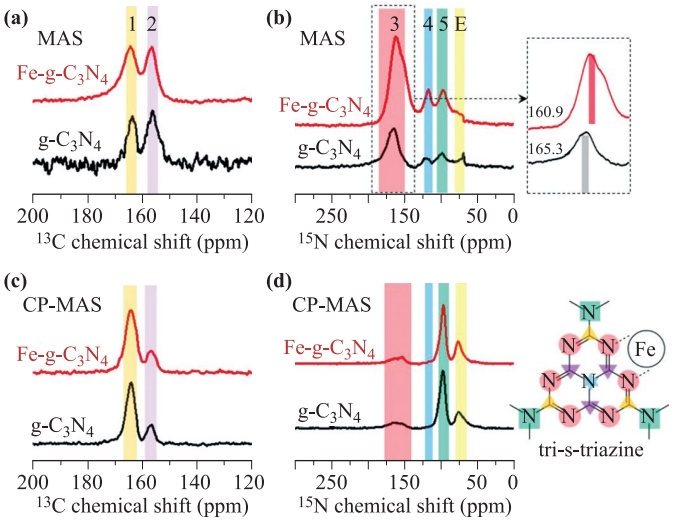

Fig. 10 Solid-state ^{13}C **(a)** and ^{15}N **(b)** magic angle spinning NMR spectra of g-C_3N_4 and Fe-g-C_3N_4. Cross-polarization magic angle spinning (CP-MAS) setup in **(c)** ^{13}C and **(d)** ^{15}N for g-C_3N_4 and Fe-g-C_3N_4 [58].

g-C_3N_4 by XPS and Mn K-edge XANES spectra. Nonmetal P atoms doping in g-C_3N_4 structure for stabilizing isolated metal species is efficient tactic to obtain structurally stable single atoms on g-C_3N_4. Liu *et al.* [51] reported single Co_1–P_4 sites on the surface of g-C_3N_4 by a facile phosphidation method. XPS spectra proved that P atoms substituted C atoms of g-C_3N_4 to form stable P–N bonds. XANES spectra suggested Co atom were coordinated with four P atoms. The obtained Co_1–P_4 sites greatly suppressed the recombination of photogenerated charge carriers in g-C_3N_4, and improved the H_2O adsorption and activation. As a result, the g-C_3N_4 with Co_1–P_4 active sites exhibited high activity in photocatalytic overall water splitting.

The single-atom metal coordinated with the N atoms in the g-C_3N_4 can greatly influence the intrinsic band structure of g-C_3N_4, and bring change of physicochemical property [9, 62, 74, 75]. Li *et al.* [63] reported single-atom Pt modified g-C_3N_4 for photocatalytic H_2 generation. The introduction of Pt can realize metal-to-ligand charge transfer (MLCT) between Pt and g-C_3N_4. As shown in Fig. 11(a), a new hybrid HOMO can be obtained after single-atom Pt modification. The MLCT process can absorb photons with energy greater than 1.8 eV [Fig. 11(b)]. Figure 11(c) exhibits the photoexcited charge density transition from Pt-induced hybrid HOMO to the LUMO of Pt modified g-C_3N_4. The new MLCT broadens the light absorption of g-C_3N_4, and then improves the visible-near-infrared photocatalytic H_2 generation activity.

The single-atom modification on g-C_3N_4 can greatly improve the seperation efficiency of photogenerated charge carriers, which is beneficial for the photocatalytic reactions [9, 51, 76, 77]. Cao *et al.* [78] found that the single-atom Pd cannot only act as active sites for photocatalytic H_2 generation, but also directional charge transfer channels for photogenerated charge carriers in g-C_3N_4. As shown in Fig. 12(a), the single-atom Pd intercalated

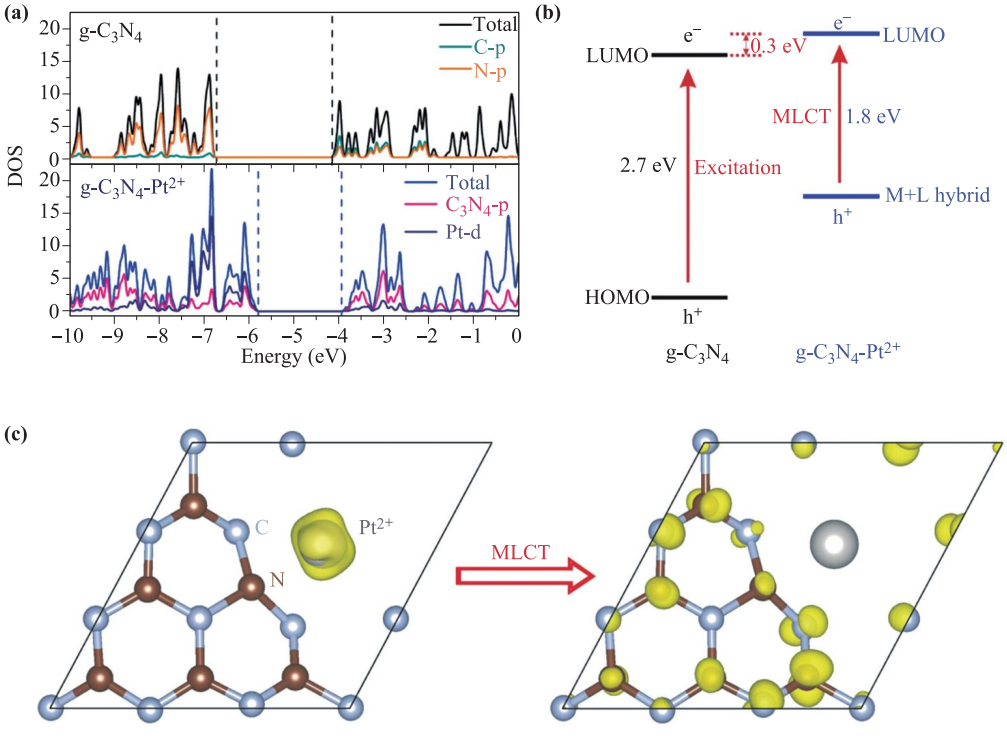

Fig. 11 DOS **(a)** and band alignment **(b)** of g-C_3N_4 and Pt^{2+} modified g-C_3N_4. **(c)** Photoexcited MLCT process from the Pt^{2+}-induced hybrid HOMO states to the LUMO of g-C_3N_4-Pt^{2+}. The yellow bubble represents electron population [63].

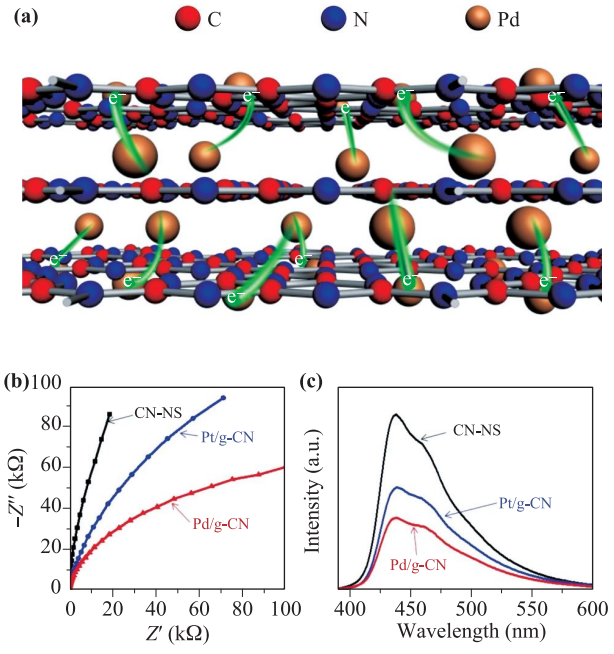

Fig. 12 **(a)** Schematic diagram of Pd atoms intercalated and surface anchored on Pd/g-CN hybrid. **(b)** Electrochemical impedance spectra (EIS) Nyquist plots of g-C_3N_4 nanosheets (CN-NS), Pd/g-CN and Pt/g-CN hybrid electrodes. **(c)** Steady-state photoluminescence (PL) spectra of CN-NS, Pd/g-CN and Pt/g-CN hybrids [78].

between layers as a bridge for electron transport, providing a new charge transfer channel. Figures 12(b) and (c) exhibit that the transfer efficiency of photogenerated charge carriers greatly improved. As a result, better photocatalytic H_2 generation activity can be obtained after single-atom Pd anchored on g-C_3N_4.

The strong interaction between single-atom metals and g-C_3N_4 not only affects the intrinsic property of g-C_3N_4, but also changes the electronic structure of the single-atom metal itself, thus affecting the intrinsic catalytic activity of the metal active site. Cao *et al.* [79] reported single-atom Pt anchored on g-C_3N_4 with stable Pt_1–N_4 moiety for photocatalytic H_2 generation. The strong interaction of Pt atoms with N atoms in g-C_3N_4 changed the distribution of Pt valence electrons, and obtained more unoccupied 5d orbitals of Pt atoms. The more unoccupied 5d orbitals of Pt can result in the shift of d-band center, and then optimize the binding energy of H and lowers absorption free energy (ΔG_{H*}), which is associated with H_2-evolution activity. Compared with Pt nanoclusters modified g-C_3N_4, the g-C_3N_4 with Pt_1–N_4 active sites exhibited more efficient photocatalytic H_2 activity due to the optimized electronic structure of single-atom Pt.

The nature of single-atom metal active sites on the surface of g-C_3N_4 has also been explored by theoretical calculations [18, 42, 80–83]. Cao *et al.* [64] studied the energy profile and reaction pathway of photocatalytic H_2 generation on the Co_1–N_4 active sites of g-C_3N_4 by DFT calculation. As shown in Fig. 13(a), the 3H atoms co-adsorption models exhibited 0.11 eV energy barrier and a highly exothermic of 0.82 eV, while 2H atoms co-adsorption models were 0.63 and 0.49 eV, respectively. This result indicated that H_2 generation on 3H atoms co-adsorption models is both kinetically and thermodynamically easier than that on the 2H atoms co-adsorption models. Figure 13(b) exhibited the formation process of H_2 on Co_1–N_4 active sites. Three H atoms adsorb on Co atom and two neighboring N atoms. The H* on N atom can transfer to bond with the adjacent H* on Co atom, and form H–H bond to release H_2 molecule. The photogenerated electron transfer from coordinated N atoms to Co atoms increased the electron density of Co, and reduced the energy barrier of Co–H intermediate, which greatly accelerated H–H coupling to H_2 generation.

In addition to single-atom metals, nonmetal single-atom B anchored on g-C_3N_4 is also one of the potential pho-

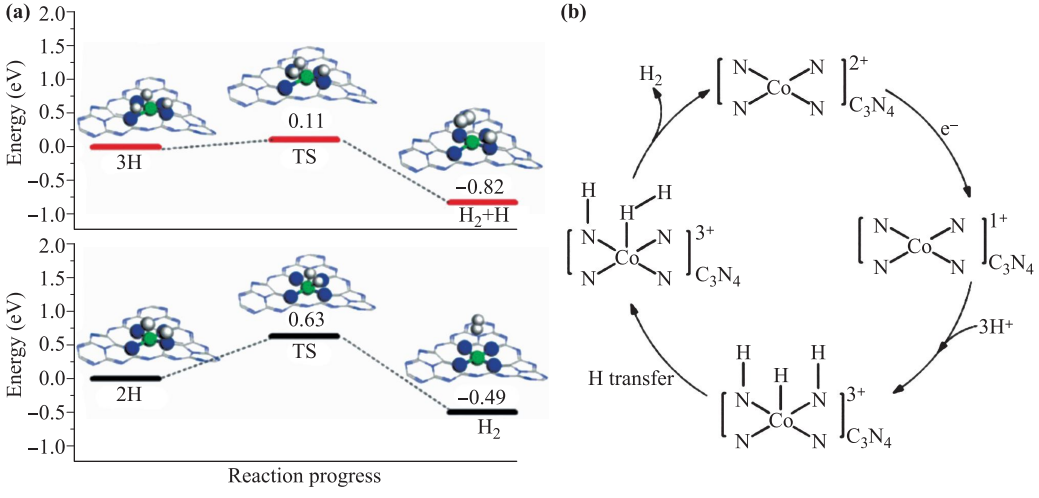

Fig. 13 **(a)** The calculated reaction barriers of 3H atoms and 2H co-adsorption models. **(b)** Proposed photocatalytic H_2 evolution process on single-site Co_1–N_4 (N blue, Co green, H white spheres) [64].

tocatalysts [84]. Ling *et al.* [10] investigated single-atom B decorated on g-C_3N_4 for photocatalytic N_2 fixation by first-principles calculations. As shown in Fig. 14(a), transition metals centers (TM Center) can act as active sites for nitrogen fixation is due to the coexistence of empty and occupied d orbitals. The empty d orbitals can accommodate the lone electron pair of N atom in N_2 molecule. The occupied d orbitals can provide electron to the antibonding orbital N_2 molecule, thus activating N≡N bonds and enhancing nitrogen fixation performance. Nonmetal B atom with sp^3 hybridization [Figs. 14(b) and (c)] contains both empty and occupied orbitals, which is potential in N_2 fixation [Fig. 14(d)]. Theoretical calculation showed that B/g-C_3N_4 can effectively reduce N_2 into NH_3 through the enzymatic mechanism at a very low initial potential (0.20 V). Moreover, single-atom B modification can significantly enhance the visible light absorption of g-C_3N_4, so it is expected to realize the solar-driven nitrogen fixation reaction.

5 Conclusion and perspectives

To date, g-C_3N_4-based single-atom photocatalysts have been widely applied in various photocatalytic applications. The advanced preparation method and characterizations are the key to develop efficient single-atom photocatalyst. Low metal precursor loading, abundant anchor sites and strong interaction between the g-C_3N_4 supports and single atoms are necessary conditions for obtaining stable single-atom g-C_3N_4 photocatalysts. The identification and action of active sites in photocatalysts are the decisive step in understanding the photocatalytic mechanism. In this review, the main preparation method and characterizations are summarized, providing some general guidelines for further development and characterization of single-atom photocatalysts. The main roles of single atoms in photocatalytic reactions, including the interactions with g-C_3N_4 supports, are also reviewed in detail. The intrinsic band structure of g-C_3N_4 support can be tuned by single-atom loading, improving the light efficiency and seperation efficiency of photogenerated charge carriers. The strong interaction between single-atom metals and g-C_3N_4 support can greatly improve the intrinsic catalytic activity of the metal active sites. Although many single-atom g-C_3N_4 photocatalysts have been reported and characterized, the mechanism of high catalytic activity is still in their infancy. There are still plenty of challenges to be resolved in this area. Some typical issues are listed below:

(1) The anchoring process of single atom on g-C_3N_4

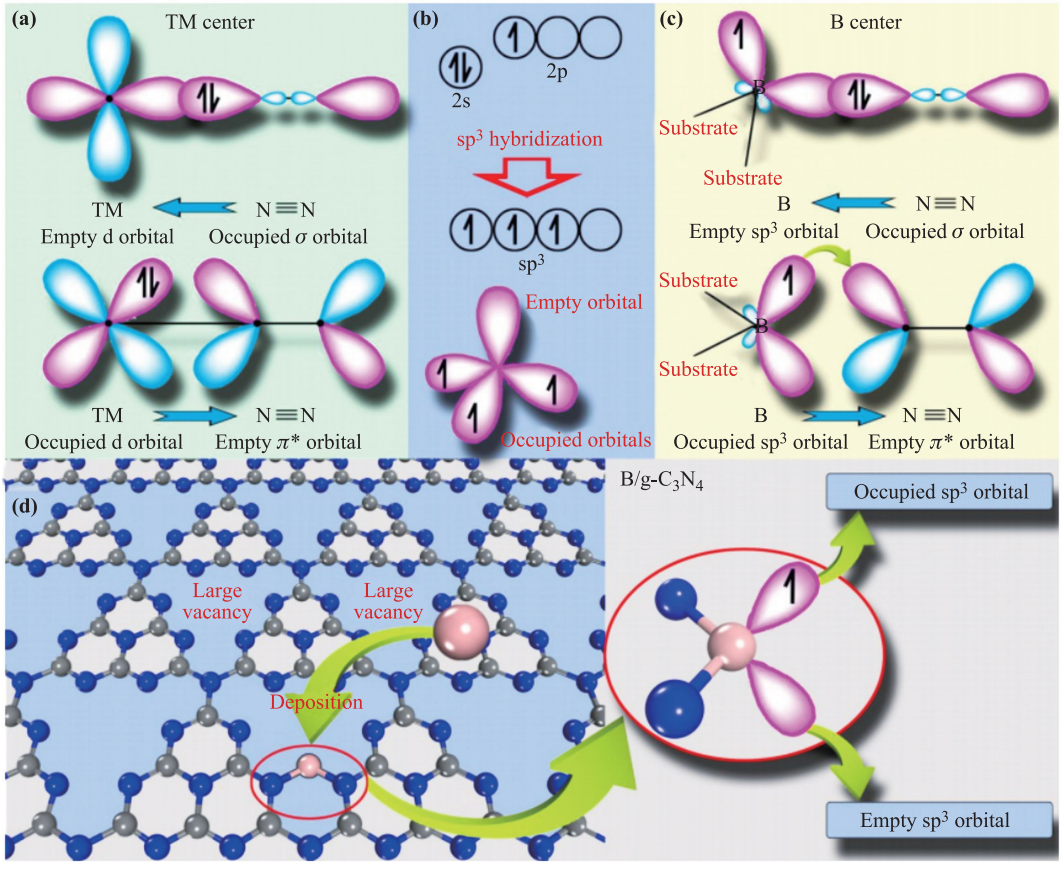

Fig. 14 **(a)** N_2 bonding to transition metals. **(b)** Electronic configuration of pure B atom and B atom with sp^3 hybridization. **(c)** N_2 binding to B atoms. **(d)** Schematic diagram of single-atom on g-C_3N_4 for photocatalytic N_2 fixation [10].

support should be thoroughly analysed. Characterizations have proved that various preparation methods are able to obtain single atoms on g-C_3N_4. However, simple and efficient strategy to prepare high-loading single atoms on g-C_3N_4 is still lacking. Understanding the whole anchoring process is using for developing and optimising the preparation methods of single atom on g-C_3N_4 support.

(2) Actual active sites of single-atom g-C_3N_4-based photocatalysts should be identify. The g-C_3N_4 support is a star photocatalyst. Many studies have shown that the two-coordinated N atoms is the main active sites for photocatalytic reactions. Single-atom metals are generally anchored by N atoms in g-C_3N_4 supports, and M–N_x (M = single-atom metals) moiety can be formed. They are the actual active sites during photocatalytic reactions, the M–N_x, or surrounding N atoms or the single metal atom. Generally, during the process of photocatalytic CO_2 reduction, C_2 products need multi-site synergism. Single-atom sites are usually single active site, it is difficult to obtain C_2 product. At present, many reported single-atom photocatalysts can only produce C_1 products in photocatalytic CO_2 reduction, such as CO, CH_4, HCOOH, and CH_3OH. The high activity of single-atom sites is a great advantage of single-atom photocatalysts. However, the single-site is difficult to achieve complex multi-site reactions. Different types of single atoms have characteristic selectivity for different reactions. It is one of the potential strategies to implement complex multi-site tandem reactions by loading two or more different kinds of single-atom sites.

(3) The interactions between single-atom metals and g-C_3N_4 support should be highlighted, which is an important indicator for stable single-atom metal on support. More importantly, the strong interactions can well regulate the electronic structure of the metal, affecting the d-band centre through electron transfer between the metal and support. The shift of d-band centre further adjusts the adsorption properties of reactants and intermediates, and finally affect the catalytic activity of metal active sites [85].

(4) More advanced in-situ characterization techniques should be developed to better study and understand the photocatalytic mechanisms. For example, in-site STM can directly observe the morphology and structure changes of photocatalysts during the reactions; in-site XAFS can study the real-time chemical environment change around the particularly interested atoms; in-site FTIR spectra can investigate the conversion of different intermediate products in catalytic process.

Acknowledgements This work was supported by the National Postdoctoral Program for Innovative Talents of China, China Postdoctoral Science Foundation (No. 2018M640759), the National Natural Science Foundation of China (Grant Nos. 21872174 and U1932148), the Project of Innovation-Driven Plan in Central South University (No. 20180018050001), the International S&T Cooperation Program of China (No. 2017YFE0127800), Hunan Provincial Science and Technology Program (No. 2017XK2026), State Key Laboratory of Powder Metallurgy, Shenzhen Science and Technology Innovation Project (No. JCYJ20180307151313532), the Hunan Provincial Science and Technology Plan Project (No. 2017TP1001), and Thousand Youth Talents Plan of China and Hundred Youth Talents Program of Hunan.

References

1. L. Jiao and H. L. Jiang, Metal-organic-framework-based single-atom catalysts for energy applications, *Chem* 5(4), 786 (2019)
2. A. Liu, K. Liu, H. Zhou, H. Li, X. Qiu, Y. Yang, and M. Liu, Solution evaporation processed high quality perovskite films, *Sci. Bull.* 63(23), 1591 (2018)
3. A. Alarawi, V. Ramalingam, and J. H. He, Recent advances in emerging single atom confined two-dimensional materials for water splitting applications, *Mater. Today Energy* 11, 1 (2019)
4. X. Wang, K. Maeda, A. Thomas, K. Takanabe, G. Xin, J. M. Carlsson, K. Domen, and M. Antonietti, A metal-free polymeric photocatalyst for hydrogen production from water under visible light, *Nat. Mater.* 8(1), 76 (2009)
5. J. Fu, K. Liu, K. Jiang, H. Li, P. An, W. Li, N. Zhang, H. Li, X. Xu, H. Zhou, D. Tang, X. Wang, X. Qiu, and M. Liu, Graphitic carbon nitride with dopant induced charge localization for enhanced photoreduction of CO_2 to CH_4, *Adv. Sci.* 6(18), 1900796 (2019)
6. J. Fu, Q. Xu, J. Low, C. Jiang, and J. Yu, Ultrathin 2D/2D WO_3/g-C_3N_4 step-scheme H_2-production photocatalyst, *Appl. Catal. B* 243, 556 (2019)
7. J. Fu, C. Bie, B. Cheng, C. Jiang, and J. Yu, Hollow CoS_x polyhedrons act as high-efficiency cocatalyst for enhancing the photocatalytic hydrogen generation of g-C_3N_4, *ACS Sustain. Chem. & Eng.* 6(2), 2767 (2018)
8. P. Huang, W. Liu, Z. He, C. Xiao, T. Yao, Y. Zou, C. Wang, Z. Qi, W. Tong, B. Pan, S. Wei, and Y. Xie, Single atom accelerates ammonia photosynthesis, *Sci. China Chem.* 61(9), 1187 (2018)
9. M. Ou, S. Wan, Q. Zhong, S. Zhang, and Y. Wang, Single Pt atoms deposition on g-C_3N_4 nanosheets for photocatalytic H_2 evolution or NO oxidation under visible light, *Int. J. Hydrogen Energy* 42(44), 27043 (2017)
10. C. Ling, X. Niu, Q. Li, A. Du, and J. Wang, Metal-free single atom catalyst for N_2 fixation driven by visible light, *J. Am. Chem. Soc.* 140(43), 14161 (2018)
11. F. Zeng, W. Q. Huang, J. H. Xiao, Y. Y. Li, W. Peng, W. Hu, K. Li, and G. F. Huang, Isotype heterojunction g-C_3N_4/g-C_3N_4 nanosheets as 2D support to highly dispersed 0D metal oxide nanoparticles: Generalized self-assembly and its high photocatalytic activity, *J. Phys. D Appl. Phys.* 52(2), 025501 (2019)
12. H. He, J. Li, Y. Liu, Q. Liu, F. Zhan, Y. Li, W. Li, and J. Wen, S-C_3N_4 quantum dot decorated ZnO nanorods to improve their photoelectrochemical performance, *Nano* 12(05), 1750064 (2017)

13. Y. Y. Li, S. F. Ma, B. X. Zhou, W. Q. Huang, X. Fan, X. Li, K. Li, and G. F. Huang, Hydroxy-carbonate-assisted synthesis of high porous graphitic carbon nitride with broken of hydrogen bonds as a highly efficient visible-light-driven photocatalyst, *J. Phys. D Appl. Phys.* 52(10), 105502 (2019)
14. J. Fu, J. Yu, C. Jiang, and B. Cheng, g-C_3N_4-based heterostructured photocatalysts, *Adv. Energy Mater.* 8(3), 1701503 (2018)
15. J. Fu, K. Jiang, X. Qiu, J. Yu, and M. Liu, Product selectivity of photocatalytic CO_2 reduction reactions, *Mater. Today* (2019), doi: 10.1016/j.mattod.2019.06.009 (in press)
16. Q. Wang, D. Zhang, Y. Chen, W. F. Fu, and X. J. Lv, Single-atom catalysts for photocatalytic reactions, *ACS Sustain. Chem. & Eng.* 7(7), 6430 (2019)
17. Y. Zhu, T. Wang, T. Xu, Y. Li, and C. Wang, Size effect of Pt co-catalyst on photocatalytic efficiency of g-C_3N_4 for hydrogen evolution, *Appl. Surf. Sci.* 464, 36 (2019)
18. J. Li, P. Yan, K. Li, J. You, H. Wang, W. Cui, W. Cen, Y. Chu, and F. Dong, Cu supported on polymeric carbon nitride for selective CO_2 reduction into CH_4: A combined kinetics and thermodynamics investigation, *J. Mater. Chem. A Mater. Energy Sustain.* 7(28), 17014 (2019)
19. C. Jin, C. Xu, W. Chang, X. Ma, X. Hu, E. Liu, and J. Fan, Bimetallic phosphide NiCoP anchored g-C_3N_4 nanosheets for efficient photocatalytic H_2 evolution, *J. Alloys Compd.* 803, 205 (2019)
20. H. Zhang, X. Han, H. Yu, Y. Zou, and X. Dong, Enhanced photocatalytic performance of boron and phosphorous co-doped graphitic carbon nitride nanosheets for removal of organic pollutants, *Separ. Purif. Tech.* 226, 128 (2019)
21. J. Li, D. Wu, J. Iocozzia, H. Du, X. Liu, Y. Yuan, W. Zhou, Z. Li, Z. Xue, and Z. Lin, Achieving efficient incorporation of π-electrons into graphitic carbon nitride for markedly improved hydrogen generation, *Angew. Chem. Int. Ed.* 58(7), 1985 (2019)
22. Y. Jiang, Z. Sun, C. Tang, Y. Zhou, L. Zeng, and L. Huang, Enhancement of photocatalytic hydrogen evolution activity of porous oxygen doped g-C_3N_4 with nitrogen defects induced by changing electron transition, *Appl. Catal. B* 240, 30 (2019)
23. J. Mao, Y. Wang, Z. Zheng, and D. Deng, The rise of two-dimensional MoS_2 for catalysis, *Front. Phys.* 13(4), 138118 (2018)
24. F. Zeng, W. Q. Huang, J. H. Xiao, Y. Y. Li, W. Peng, W. Hu, K. Li, and G. F. Huang, Isotype heterojunction g-C_3N_4/g-C_3N_4 nanosheets as 2D support to highly dispersed 0D metal oxide nanoparticles: Generalized self-assembly and its high photocatalytic activity, *J. Phys. D: Appl. Phys.* 52(2), 025501 (2019)
25. S. S. Ding, W. Q. Huang, Y. C. Yang, B. X. Zhou, W. Y. Hu, M. Q. Long, P. Peng, and G. F. Huang, Dual role of monolayer MoS_2 in enhanced photocatalytic performance of hybrid MoS_2/SnO_2 nanocomposite, *J. Appl. Phys.* 119(20), 205704 (2016)
26. X. Ren, X. Qi, Y. Shen, S. Xiao, G. Xu, Z. Zhang, Z. Huang, and J. Zhong, 2D co-catalytic MoS_2 nanosheets embedded with 1D TiO_2 nanoparticles for enhancing photocatalytic activity, *J. Phys. D Appl. Phys.* 49(31), 315304 (2016)
27. D. Xu, S. Wang, B. Wu, B. Zhang, Y. Qin, C. Huo, L. Huang, X. Wen, Y. Yang, and Y. Li, Highly dispersed single-atom Pt and Pt clusters in the Fe-modified kl zeolite with enhanced selectivity for n-heptane aromatization, *ACS Appl. Mater. Inter.* 11(33), 29858 (2019)
28. A. Wang, J. Li, and T. Zhang, Heterogeneous single-atom catalysis, *Nat. Rev. Chem.* 2(6), 65 (2018)
29. Z. Chen, E. Vorobyeva, S. Mitchell, E. Fako, N. Lopez, S. M. Collins, R. K. Leary, P. A. Midgley, R. Hauert, and J. Perez-Ramirez, Single-atom heterogeneous catalysts based on distinct carbon nitride scaffolds, *Natl. Sci. Rev.* 5(5), 642 (2018)
30. Z. Chen, J. Zhang, S. Zheng, J. Ding, J. Sun, M. Dong, M. Abbas, Y. Chen, Z. Jiang, and J. Chen, The texture evolution of g-C_3N_4 nanosheets supported Fe catalyst during Fischer-Tropsch synthesis, *Mol. Catal.* 444, 90 (2018)
31. J. Di, C. Chen, S. Z. Yang, S. Chen, M. Duan, J. Xiong, C. Zhu, R. Long, W. Hao, Z. Chi, H. Chen, Y. X. Weng, J. Xia, L. Song, S. Li, H. Li, and Z. Liu, Isolated single atom cobalt in Bi_3O_4Br atomic layers to trigger efficient CO_2 photoreduction, *Nat. Commun.* 10(1), 2840 (2019)
32. Z. Ma, J. Zhuang, X. Zhang, and Z. Zhou, SiP monolayers: New 2D structures of group IV-V compounds for visible-light photohydrolytic catalysts, *Front. Phys.* 13(3), 138104 (2018)
33. P. Huang, J. Huang, S. A. Pantovich, A. D. Carl, T. G. Fenton, C. A. Caputo, R. L. Grimm, A. I. Frenkel, and G. Li, Selective CO_2 reduction catalyzed by single cobalt sites on carbon nitride under visible-light irradiation, *J. Am. Chem. Soc.* 140(47), 16042 (2018)
34. T. He, C. Zhang, L. Zhang, and A. Du, Single Pt atom decorated graphitic carbon nitride as an efficient photocatalyst for the hydrogenation of nitrobenzene into aniline, *Nano Res.* 12(8), 1817 (2019)
35. B. C. Gates, M. Flytzani-Stephanopoulos, D. A. Dixon, and A. Katz, Atomically dispersed supported metal catalysts: Perspectives and suggestions for future research, *Catal. Sci. Technol.* 7(19), 4259 (2017)
36. J. Liu, Catalysis by supported single metal atoms, *ACS Catal.* 7(1), 34 (2017)
37. X. F. Yang, A. Wang, B. Qiao, J. Li, J. Liu, and T. Zhang, Single-atom catalysts: A new frontier in heterogeneous catalysis, *Acc. Chem. Res.* 46(8), 1740 (2013)
38. J. Di, J. Xiong, H. Li, and Z. Liu, Ultrathin 2D photocatalysts: Electronic-structure tailoring, hybridization, and applications, *Adv. Mater.* 30(1), 1704548 (2018)
39. B. Zhang, T. Fan, N. Xie, G. Nie, and H. Zhang, Versatile applications of metal single-atom@2D material nanoplatforms, *Adv. Sci.* 6(21), 1901787 (2019)
40. J. Liu, B. R. Bunes, L. Zang, and C. Wang, Supported single-atom catalysts: synthesis, characterization, properties, and applications, *Environ. Chem. Lett.* 16(2), 477 (2018)

41. L. Wang, L. Huang, F. Liang, S. Liu, Y. Wang, and H. Zhang, Preparation, characterization and catalytic performance of single-atom catalysts, *Chin. J. Catal.* 38(9), 1528 (2017)
42. S. L. Li, H. Yin, X. Kan, L. Y. Gan, U. Schwingenschlogl, and Y. Zhao, Potential of transition metal atoms embedded in buckled monolayer g-C_3N_4 as single-atom catalysts, *Phys. Chem. Chem. Phys.* 19(44), 30069 (2017)
43. Y. Li, T. Kong, and S. Shen, Artificial photosynthesis with polymeric carbon nitride: When meeting metal nanoparticles, single atoms, and molecular complexes, *Small* 15(32), 1900772 (2019)
44. Z. Chen, S. Mitchell, E. Vorobyeva, R. K. Leary, R. Hauert, T. Furnival, Q. M. Ramasse, J. M. Thomas, P. A. Midgley, D. Dontsova, M. Antonietti, S. Pogodin, N. López, and J. Pérez-Ramírez, Stabilization of single metal atoms on graphitic carbon nitride, *Adv. Funct. Mater.* 27(8), 1605785 (2017)
45. G. Vilé, D. Albani, M. Nachtegaal, Z. Chen, D. Dontsova, M. Antonietti, N. Lopez, and J. Perez-Ramirez, A stable single-site palladium catalyst for hydrogenations, *Angew. Chem. Int. Ed.* 54(38), 11265 (2015)
46. S. Tian, Z. Wang, W. Gong, W. Chen, Q. Feng, Q. Xu, C. Chen, C. Chen, Q. Peng, L. Gu, H. Zhao, P. Hu, D. Wang, and Y. Li, Temperature-controlled selectivity of hydrogenation and hydrodeoxygenation in the conversion of biomass molecule by the Ru_1/mpg-C_3N_4 catalyst, *J. Am. Chem. Soc.* 140(36), 11161 (2018)
47. X. Li, W. Bi, L. Zhang, S. Tao, W. Chu, Q. Zhang, Y. Luo, C. Wu, and Y. Xie, Single-atom Pt as co-catalyst for enhanced photocatalytic H_2 evolution, *Adv. Mater.* 28(12), 2427 (2016)
48. Z. Chen, Q. Zhang, W. Chen, J. Dong, H. Yao, X. Zhang, X. Tong, D. Wang, Q. Peng, C. Chen, W. He, and Y. Li, Single-site Au-I catalyst for silane oxidation with water, *Adv. Mater.* 30(5), 1704720 (2018)
49. L. Liu, H. Su, F. Tang, X. Zhao, and Q. Liu, Confined organometallic Au_1N_x single-site as an efficient bifunctional oxygen electrocatalyst, *Nano Energy* 46, 110 (2018)
50. Z. Chen, S. Mitchell, F. Krumeich, R. Hauert, S. Yakunin, M. V. Kovalenko, and J. Perez-Ramirez, Tunability and scalability of single-atom catalysts based on carbon nitride, *ACS Sustain. Chem. & Eng.* 7(5), 5223 (2019)
51. W. Liu, L. Cao, W. Cheng, Y. Cao, X. Liu, W. Zhang, X. Mou, L. Jin, X. Zheng, W. Che, Q. Liu, T. Yao, and S. Wei, Single-site active cobalt-based photocatalyst with a long carrier lifetime for spontaneous overall water splitting, *Angew. Chem. Int. Ed.* 56(32), 9312 (2017)
52. P. Zhou, F. Lv, N. Li, Y. Zhang, Z. Mu, Y. Tang, J. Lai, Y. Chao, M. Luo, F. Lin, J. Zhou, D. Su, and S. Guo, Strengthening reactive metal-support interaction to stabilize high-density Pt single atoms on electron-deficient g-C_3N_4 for boosting photocatalytic H_2 production, *Nano Energy* 56, 127 (2019)
53. X. Han, X. Ling, Y. Wang, T. Ma, C. Zhong, W. Hu, and Y. Deng, Generation of nanoparticle, atomic-cluster, and single-atom cobalt catalysts from zeolitic imidazole frameworks by spatial isolation and their use in zinc-air batteries, *Angew. Chem. Int. Ed.* 58(16), 5359 (2019)
54. F. Dubray, S. Moldovan, C. Kouvatas, J. Grand, C. Aquino, N. Barrier, J. P. Gilson, N. Nesterenko, D. Minoux, and S. Mintova, Direct evidence for single molybdenum atoms incorporated in the framework of MFI zeolite nanocrystals, *J. Am. Chem. Soc.* 141(22), 8689 (2019)
55. Q. Feng, S. Zhao, Q. Xu, W. Chen, S. Tian, Y. Wang, W. Yan, J. Luo, D. Wang, and Y. Li, Mesoporous nitrogen-doped carbon-nanosphere-supported isolated single-atom Pd catalyst for highly efficient semihydrogenation of acetylene, *Adv. Mater.* 31(36), 1901024 (2019)
56. H. Wei, K. Huang, D. Wang, R. Zhang, B. Ge, J. Ma, B. Wen, S. Zhang, Q. Li, M. Lei, C. Zhang, J. Irawan, L. M. Liu, and H. Wu, Iced photochemical reduction to synthesize atomically dispersed metals by suppressing nanocrystal growth, *Nat. Commun.* 8(1), 1490 (2017)
57. P. Liu, Y. Zhao, R. Qin, S. Mo, G. Chen, L. Gu, D. M. Chevrier, P. Zhang, Q. Guo, D. Zang, B. Wu, G. Fu, and N. Zheng, Photochemical route for synthesizing atomically dispersed palladium catalysts, *Science* 352(6287), 797 (2016)
58. Y. Oh, J. O. Hwang, E. S. Lee, M. Yoon, V. D. Le, Y. H. Kim, D. H. Kim, and S. O. Kim, Divalent Fe atom coordination in two-dimensional microporous graphitic carbon nitride, *ACS Appl. Mater. Interfaces* 8(38), 25438 (2016)
59. H. Li, Y. Xia, T. Hu, Q. Deng, N. Du, and W. Hou, Enhanced charge carrier separation of manganese(ii)-doped graphitic carbon nitride: Formation of N–Mn bonds through redox reactions, *J. Mater. Chem. A Mater. Energy Sustain.* 6(15), 6238 (2018)
60. Z. Chen, S. Pronkin, T. P. Fellinger, K. Kailasam, G. Vile, D. Albani, F. Krumeich, R. Leary, J. Barnard, J. M. Thomas, J. Perez-Ramirez, M. Antonietti, and D. Dontsova, Merging single-atom-dispersed silver and carbon nitride to a joint electronic system via copolymerization with silver tricyanomethanide, *ACS Nano* 10(3), 3166 (2016)
61. F. Wang, Y. Wang, Y. Li, X. Cui, Q. Zhang, Z. Xie, H. Liu, Y. Feng, W. Lv, and G. Liu, The facile synthesis of a single atom-dispersed silver-modified ultrathin g-C_3N_4 hybrid for the enhanced visible-light photocatalytic degradation of sulfamethazine with peroxymonosulfate, *Dalton Trans.* 47(20), 6924 (2018)
62. F. Wang, Y. Wang, Y. Feng, Y. Zeng, Z. Xie, Q. Zhang, Y. Su, P. Chen, Y. Liu, K. Yao, W. Lv, and G. Liu, Novel ternary photocatalyst of single atom-dispersed silver and carbon quantum dots co-loaded with ultrathin g-C_3N_4 for broad spectrum photocatalytic degradation of naproxen, *Appl. Catal. B* 221, 510 (2018)
63. Y. Li, Z. Wang, T. Xia, H. Ju, K. Zhang, R. Long, Q. Xu, C. Wang, L. Song, J. Zhu, J. Jiang, and Y. Xiong, Implementing metal-to-ligand charge transfer in organic semiconductor for improved visible-near-infrared photocatalysis, *Adv. Mater.* 28(32), 6959 (2016)
64. Y. Cao, S. Chen, Q. Luo, H. Yan, Y. Lin, W. Liu, L. Cao, J. Lu, J. Yang, T. Yao, and S. Wei, Atomic-level insight into optimizing the hydrogen evolution pathway over a Co_1N_4 single-site photocatalyst, *Angew. Chem. Int. Ed.* 56(40), 12191 (2017)

65. A. Kumar, P. K. Prajapati, M. S. Aathira, A. Bansiwal, R. Boukherroub, and S. L. Jain, Highly improved photoreduction of carbon dioxide to methanol using cobalt phthalocyanine grafted to graphitic carbon nitride as photocatalyst under visible light irradiation, *J. Colloid Interface Sci.* 543, 201 (2019)
66. T. Shi, H. Li, L. Ding, F. You, L. Ge, Q. Liu, and K. Wang, Facile preparation of unsubstituted iron(ii) phthalocyanine/carbon nitride nanocomposites: A multipurpose catalyst with reciprocally enhanced photo/electrocatalytic activity, *ACS Sustain. Chem. & Eng.* 7(3), 3319 (2019)
67. T. Xu, D. Wang, L. Dong, H. Shen, W. Lu, and W. Chen, Graphitic carbon nitride co-modified by zinc phthalocyanine and graphene quantum dots for the efficient photocatalytic degradation of refractory contaminants, *Appl. Catal. B* 244, 96 (2019)
68. T. Zheng, K. Jiang, N. Ta, Y. Hu, J. Zeng, J. Liu, and H. Wang, Large-scale and highly selective CO_2 electrocatalytic reduction on nickel single-atom catalyst, *Joule* 3(1), 265 (2019)
69. H. Yang, Y. Wu, G. Li, Q. Lin, Q. Hu, Q. Zhang, J. Liu, and C. He, Scalable production of efficient single-atom copper decorated carbon membranes for CO_2 electroreduction to methanol, *J. Am. Chem. Soc.* 141(32), 12717 (2019)
70. H. Yang, L. Shang, Q. Zhang, R. Shi, G. I. N. Waterhouse, L. Gu, and T. Zhang, A universal ligand mediated method for large scale synthesis of transition metal single atom catalysts, *Nat. Commun.* 10(1), 4585 (2019)
71. K. Jiang, S. Siahrostami, A. J. Akey, Y. Li, Z. Lu, J. Lattimer, Y. Hu, C. Stokes, M. Gangishetty, G. Chen, Y. Zhou, W. Hill, W. B. Cai, D. Bell, K. Chan, J. K. Norskov, Y. Cui, and H. Wang, Transition-metal single atoms in a graphene shell as active centers for highly efficient artificial photosynthesis, *Chem* 3(6), 950 (2017)
72. C. Asokan, L. DeRita, and P. Christopher, Using probe molecule FTIR spectroscopy to identify and characterize Pt-group metal based single atom catalysts, *Chin. J. Catal.* 38(9), 1473 (2017)
73. K. Ding, A. Gulec, A. M. Johnson, N. M. Schweitzer, G. D. Stucky, L. D. Marks, and P. C. Stair, Identification of active sites in CO oxidation and water-gas shift over supported Pt catalysts., *Science* 350(6257), 189 (2015) (2015)
74. Y. Wang, X. Zhao, D. Cao, Y. Wang, and Y. Zhu, Peroxymonosulfate enhanced visible light photocatalytic degradation bisphenol A by single-atom dispersed Ag mesoporous g-C_3N_4 hybrid, *Appl. Catal. B* 211, 79 (2017)
75. L. Liu, X. Wu, L. Wang, X. Xu, L. Gan, Z. Si, J. Li, Q. Zhang, Y. Liu, Y. Zhao, R. Ran, X. Wu, D. Weng, and F. Kang, Atomic palladium on graphitic carbon nitride as a hydrogen evolution catalyst under visible light irradiation, *Commun. Chem.* 2(1), 18 (2019)
76. G. Wu, S. Hu, Z. Han, C. Liu, and Q. Li, The effect of Ni(i)–N active sites on the photocatalytic H_2O_2 production ability over nickel doped graphitic carbon nitride nanofibers, *New J. Chem.* 41(24), 15289 (2017)
77. Q. Song, J. Li, L. Wang, Y. Qin, L. Pang, and H. Liu, Stable single-atom cobalt as a strong coupling bridge to promote electron transfer and separation in photoelectrocatalysis, *J. Catal.* 370, 176 (2019)
78. S. Cao, H. Li, T. Tong, H. C. Chen, A. Yu, J. Yu, and H. M. Chen, Single-atom engineering of directional charge transfer channels and active sites for photocatalytic hydrogen evolution, *Adv. Funct. Mater.* 28(32), 1802169 (2018)
79. Y. Cao, D. Wang, Y. Lin, W. Liu, L. Cao, X. Liu, W. Zhang, X. Mou, S. Fang, X. Shen, and T. Yao, Single Pt atom with highly vacant d-orbital for accelerating photocatalytic H_2 evolution, *ACS Appl. Energy Mater.* 1(11), 6082 (2018)
80. T. Tong, B. Zhu, C. Jiang, B. Cheng, and J. Yu, Mechanistic insight into the enhanced photocatalytic activity of single-atom Pt, Pd or Au-embedded g-C_3N_4, *Appl. Surf. Sci.* 433, 1175 (2018)
81. T. Tong, B. He, B. Zhu, B. Cheng, and L. Zhang, First-principle investigation on charge carrier transfer in transition-metal single atoms loaded g-C_3N_4, *Appl. Surf. Sci.* 459, 385 (2018)
82. H. Li, Y. Wu, L. Li, Y. Gong, L. Niu, X. Liu, T. Wang, C. Sun, and C. Li, Adjustable photocatalytic ability of monolayer g-C_3N_4 utilizing single-metal atom: Density functional theory, *Appl. Surf. Sci.* 457, 735 (2018)
83. G. Gao, Y. Jiao, E. R. Waclawik, and A. Du, Single atom (Pd/Pt) supported on graphitic carbon nitride as an efficient photocatalyst for visible-light reduction of carbon dioxide, *J. Am. Chem. Soc.* 138(19), 6292 (2016)
84. X. Lv, W. Wei, F. Li, B. Huang, and Y. Dai, Metal-free B@g-CN: Visible/infrared light-driven single atom photocatalyst enables spontaneous dinitrogen reduction to ammonia, *Nano Lett.* 19(9), 6391 (2019)
85. M. M. Millet, G. Algara-Siller, S. Wrabetz, A. Mazheika, F. Girgsdies, D. Teschner, F. Seitz, A. Tarasov, S. V. Levchenko, R. Schlögl, and E. Frei, Ni single atom catalysts for CO_2 activation, *J. Am. Chem. Soc.* 141(6), 2451 (2019)